

Development of High-performance n-Type Organic Field-effect Transistors Based on Nitrogen Heterocycles

Yoshiro Yamashita

(Received April 24, 2009; CL-098006)

Abstract

Nitrogen heterocycles containing C=N double bonds have electron-accepting properties and can be used as n-type semiconductors for organic field-effect transistors. Thiazole, benzothiadiazole, pyrazine, and related heterocycles have been incorporated in π -conjugated systems. The effects of the structures and electron affinity of the heterocycles on transistor characteristics have been investigated here.

1. Introduction

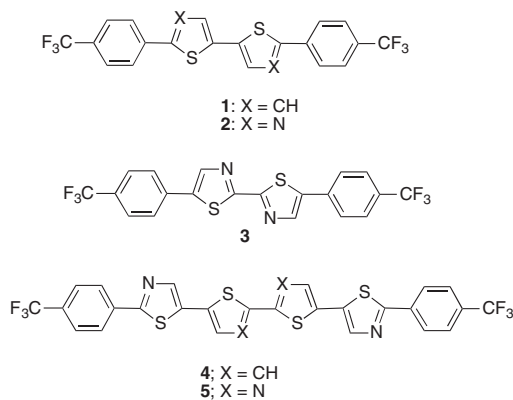
Organic field-effect transistors (OFETs) have attracted much attention for applications such as display drivers and identification tags because they have advantages of low cost, flexibility, and light weight.¹ Organic semiconductors can be processed at low temperatures compatible with plastic substrates. By using solution techniques such as spin coating, inkjet printing, and screen printing, large-area fabrication is possible at low cost. Modification of organic semiconductors can easily tune the characteristics of transistors. As mentioned above, OFETs have great possibilities in organic electronics.

FET characteristics are evaluated mainly on carrier mobility, on/off current ratio, and threshold voltage. High-performance transistors display high mobility, large on/off ratio, and low threshold voltage. In addition, high stability of the devices in air is essential for practical application. To achieve such high performance, development of new organic semiconductors as well as the improvement of device structure is very important. Many p-type organic semiconductors have been reported and some semiconductors show higher mobilities than amorphous silicon ($1 \text{ cm}^2 \text{ V}^{-1} \text{ s}^{-1}$).² On the other hand, n-type semiconductors are still not fully developed and performance is not satisfactory. The n-type semiconductors are important as key components of p-n junctions and advanced electron-transporting materials.³ To achieve high electron mobilities in FET devices, organic semiconductors should be highly ordered with strong intermolecular interactions. Proper LUMO energy levels near the work functions of source/drain electrodes are also necessary for low threshold voltages. Recently, high-performance n-type semiconductors have been obtained by introducing electron-withdrawing groups such as fluoro or perfluoroalkyl substituents into p-type semiconductor cores such as pentacene and oligothiophenes.⁴ However, they still have disadvantages of insufficient intermolecular π - π interactions and unfavorable electron

injection. These disadvantages were expected to be overcome by using electron-accepting heterocycles as the core of π -electron systems. Nitrogen-heterocycles containing C=N double bonds have electron-accepting properties and can be used for this purpose. From this viewpoint, we have developed new n-type semiconductors containing thiazole, thiadiazole, pyrazine, and related heterocycles. I will highlight here those materials giving high-performance n-type organic FETs.

2. Thiazole-containing Compounds

We have achieved high electron mobilities by using a trifluoromethylphenyl group as end substituents. Bithiophene derivative **1** with the substituents showed a high mobility of $0.18 \text{ cm}^2 \text{ V}^{-1} \text{ s}^{-1}$ which was higher than that of the corresponding perfluorohexyl derivative.⁵ This result shows that the trifluoromethylphenyl group is superior for inducing n-type semiconducting behavior probably because the group is effective to afford well-ordered crystalline films. However, the threshold voltage of the FET based on **1** was very high (76 V), and one reason considered was due to the weak electron affinity resulting in a high barrier of electron injection from electrodes. Therefore, the thiophene rings of **1** were replaced by electron-accepting thiazole rings to give **2** (Scheme 1).⁶ The electron mobility of a device using a bare SiO_2 substrate was $0.21 \text{ cm}^2 \text{ V}^{-1} \text{ s}^{-1}$, and the threshold voltage was a little decreased. The mobility was increased to $1.83 \text{ cm}^2 \text{ V}^{-1} \text{ s}^{-1}$ by using an OTS (octadecyltrichlorosilane)-modified SiO_2 substrate although the threshold voltage was increased.⁶ The output and transfer characteristics are de-



Scheme 1.

Prof. Yoshiro Yamashita

Department of Electronic Chemistry, Interdisciplinary Graduate School of Science and Engineering, Tokyo Institute of Technology, Nagatsuta, Midori-ku, Yokohama 226-8502

E-mail: yoshiro@echem.titech.ac.jp

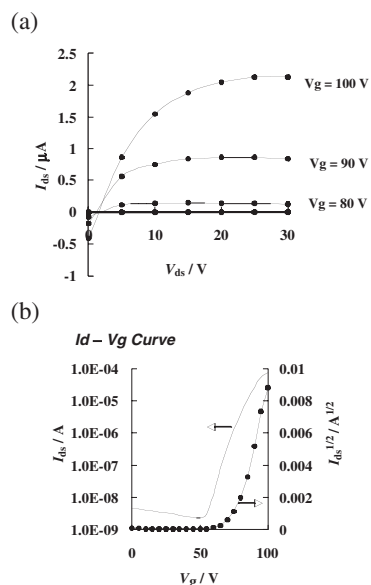


Figure 1. (a) Output characteristics and (b) transfer characteristics of the FET of **2**.

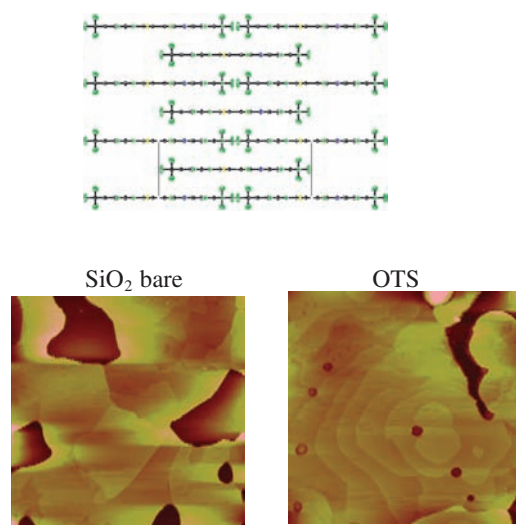
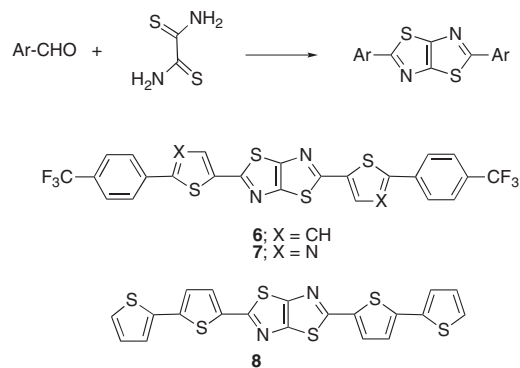


Figure 2. Crystal structure of **2** and AFM images of the films.

scribed in Figure 1. Molecule **2** in a single crystal is completely planar and forms a π -stacking structure in contrast to the herringbone structure of **1**. In addition, a two-dimensional (2-D) columnar structure was observed as shown in Figure 2, which is thought to be formed to avoid steric repulsion of CF₃ groups. The increase of the mobility on the SiO₂ surface treatment was explained by a morphology change of the films. Thus, the grain size increased after surface treatment. The AFM image of the OTS-treated film reveals a terrace-like layer structure in contrast to the bare SiO₂, leading to the high mobility in the OTS film. On the other hand, isomer **3** containing nitrogen atoms at different positions did not show any FET characteristics. Molecule **3** is a little twisted with a dihedral angle of 10.4° and forms a π -stacking structure in the single crystal. However, the XRD measurement showed no peak, indicating the disorder arrangement of molecules in the thin film. This may be attributed to the easy ro-



Scheme 2.

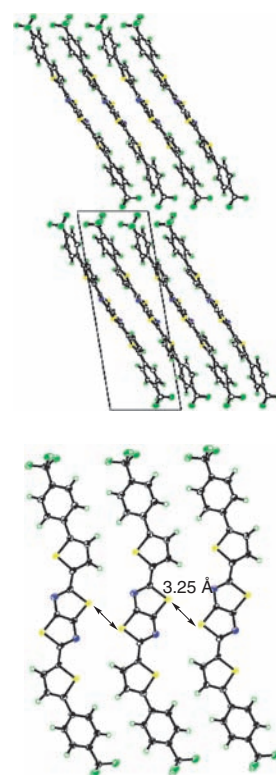


Figure 3. Crystal structure of **6** (π -stacking and short S...S contact).

tation of the central C–C bond of **3** resulting in the disorder orientation.

The system of **2** was further modified to extend π conjugation to give co-oligomers **4** and **5**.⁶ The FET performance of **4** is much better than that of **5**. The low performance of **5** is also attributed to the conformational disorder caused by the rotation of the central bond as found in **3**. To suppress this rotation and construct a more rigid system, thiazolothiazole-containing compound **6** was designed.⁵ This bicyclic ring can be easily formed by a one-step reaction of aromatic aldehydes with commercially available dithiooxamide (Scheme 2). The rigid and polarized heterocyclic system was expected to induce strong intermolecular π – π interactions. Actually, **6** has a π -stacking structure and short heteroatom contacts (S...S contact of 3.25 Å) between the columns in the crystal as shown in Figure 3, that is a kind of

Table 1. Reduction potentials and FET characteristics^a of thiazole-containing compounds

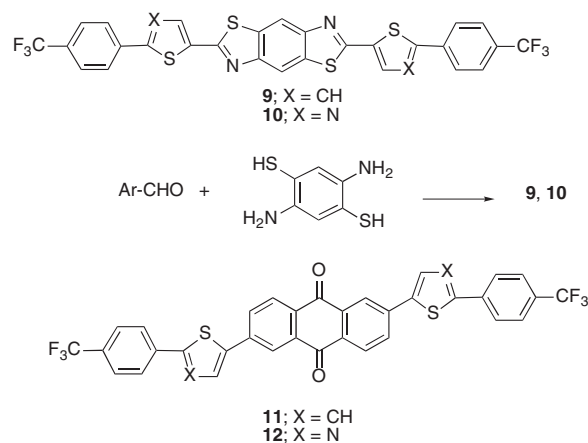
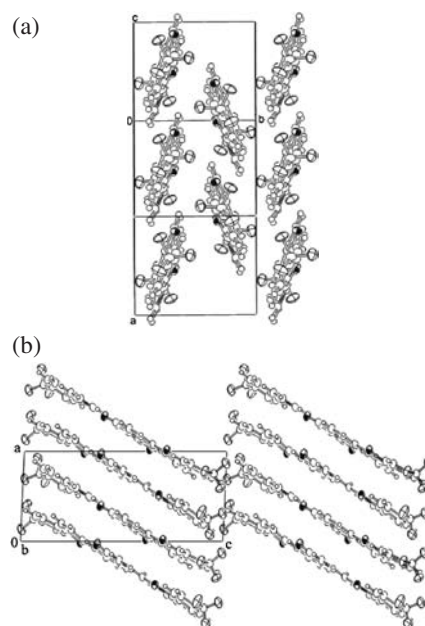
Compound	E_{red} /V ^b	Device type	Mobility / $\text{cm}^2 \text{V}^{-1} \text{s}^{-1}$	Threshold /V
1	−1.81	top	0.18	+76
2	−1.63	top	1.83	+78
3	−1.46	top	not observed	
4	−1.62	top	0.085	+63
5	−1.35	top	0.0028	+63
6	−1.48	top	1.20	+67
7	−1.08	top	0.64	+24
9	−1.40	top	0.24	+24
10	−0.99	top	0.05	+28
11	−0.88	bottom	0.020	+26
12	— ^c	bottom	0.074	+25

^aThe highest mobilities reported. ^bThe first reduction potentials, V vs. SCE. ^cNot measured due to the low solubility.

2-D structure. A similar crystal structure was observed in the bithiophene derivative **8**,⁷ suggesting that the thiazolothiazole unit is crucial for the construction of the 2-D structure. The FET device based on **6** using a bare SiO_2 substrate showed a high electron mobility of $0.30 \text{ cm}^2 \text{V}^{-1} \text{s}^{-1}$ with a threshold voltage of 60 V. On the other hand, bithiophene derivative **8** showed a p-type semiconducting behavior. This fact indicates that the CF_3 -phenyl group plays an important role in exhibiting high electron mobility.

Although optimization of the device structure based on **6** by using an OTS-modified SiO_2 substrate improved the mobility to $1.2 \text{ cm}^2 \text{V}^{-1} \text{s}^{-1}$, the threshold voltage was still high (Table 1).⁸ To decrease the threshold voltage, the LUMO levels of semiconductors should be lowered for facile electron injection. The LUMO levels can be estimated from the reduction potentials. Replacement of the thiophene rings of **6** by thiazole ones to give **7** shifts the reduction potentials positively, indicating that the electron affinity is increased by the replacement.⁹ The FET device based on **7** exhibited a lower threshold voltage of 24 V with a high mobility of $0.64 \text{ cm}^2 \text{V}^{-1} \text{s}^{-1}$ as shown in Table 1.

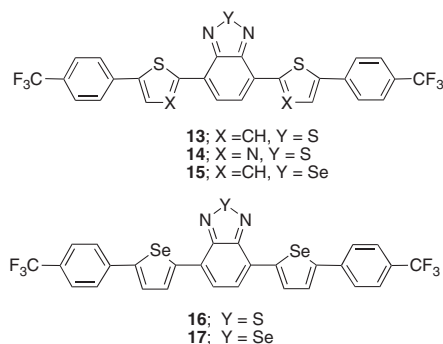
The extension of π conjugation is considered to be useful for increase in intermolecular interactions as well as decrease in Coulomb repulsion. For this purpose, benzobisthiazole derivatives **9** and **10** were designed.¹⁰ They were easily obtained by reaction of commercially available 2,5-diamino-1,4-benzenedithiol and the corresponding aldehydes (Scheme 3). The packing structure in the single crystal of **9** is a herringbone type as shown in Figure 4, which is in contrast to the π -stacking structure of **6**. This is probably due to the electron repulsion between the benzobisthiazole rings of **9**. Although the π - π intermolecular interaction is weaker in the herringbone packing than in the π -stacked one, the former is more favorable for the high dimensionality as seen in pentacene. The mobility of **9** is a little low compared to that of **6** (Table 1). However, the threshold voltage is much reduced to 24 V although the electron affinity is similar. This result may be attributed to the herringbone structure of **9** leading to a better contact between the semiconductor and the electrodes. On the other hand, the thiazole analogue **10** exhibited a poor FET performance. This result was attributed to its amorphous-like morphology in the thin film since no peak was observed in the X-ray diffraction analysis.

**Scheme 3.****Figure 4.** (a) Crystal structures of **9** and (b) **11**.

Instead of the benzobisthiazole core, anthraquinone was used since it has a high electron affinity.¹¹ The derivatives **11** and **12** afforded good performance FETs as shown in Table 1. In this case, the mobilities were better in thiazole derivative **12** than in thiophene **11**. This result is attributed to the stronger intermolecular interactions in **12** than in **11**. Their crystal structures are π stacking in contrast to the herringbone structure of **9**.¹¹ The crystal structure of **11** is described in Figure 4, which shows a one-dimensional column.

3. Benzothiadiazole and Benzoselenadiazole-containing Compounds

2,1,3-Benzothiadiazole is a stronger electron-acceptor than thiazole because of the quinoid structure as well as the two $\text{C}=\text{N}$ double bonds. The heterocyclic unit has been used in electron acceptors for organic conductors or electron-transporting materials and emission layers for organic electron-luminescence devices. The heterocycle has also been used for OFETs. Re-



Scheme 4.

Table 2. Reduction potentials and FET characteristics^a of compounds **13–17**

Compound	E_{red} /V ^b	Type	T_{sub} /°C	Mobility /cm ² V ⁻¹ s ⁻¹	Threshold /V
13	−1.00	bottom	25	5.5×10^{-5}	+35
		bottom	80	0.043	+35
		top	80	0.19	+3
14	−0.77	top	50	0.068	+15
15	−0.92	bottom	25	8.1×10^{-4}	+40
		bottom	100	0.011	+59
16	−0.91	bottom	25	0.012	+49
		bottom	100	0.19	+20
17	−0.86	bottom	25	0.061	+28
		bottom	100	0.16	+23

^aThe highest mobilities reported. ^bThe first reduction potentials, V vs. SCE.

placement of the thiazolothiazole core in **6** by the benzothiadiazole ring gives **13** (Scheme 4). The reduction potential of **13** is much higher than that of **6**, confirming the high electron affinity. The FET device based on **13** showed good mobility and low threshold voltage (Table 2).¹² Particularly, the low threshold voltage of 3 V in the top contact device is noteworthy, which can be attributed to the high electron affinity of **13**. In addition, the FET device showed n-type light-emitting FET characteristics. When Au source and drain electrodes were used, red emission of 662 nm consistent with that of fluorescence was observed near the electrode. The emission intensity increases with an increase of the gate voltage, confirming that the device is a light-emitting FET. This is due to the small HOMO–LUMO energy gap leading to direct hole injection from the electrode. On the other hand, the thiazole-substituted derivative **14** also showed good FET performance (Table 2).¹³ The single-crystal X-ray structure analysis revealed that the molecule has a short intramolecular S...N contact of 2.89 Å resulting from the electrostatic interaction, which makes the direction of the thiazole ring definite.

On the other hand, introduction of selenium atoms is expected to increase intermolecular interactions owing to the more polarized nature of the selenium atom. In this context, selenium-containing compounds **15–17** were synthesized.¹⁴ The comparison of **13** and **15** indicates that the selenadiazole ring has a higher electron affinity than the thiadiazole. The selenophene rings in **16** and **17** also decreases the LUMO energies compared with the thiophenes as seen in their reduction potentials which are more

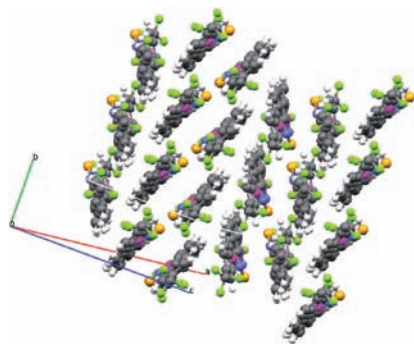
positively shifted than those of the corresponding molecules **13** and **15**. The single-crystal X-ray structure analysis of **16** reveals a multidimensional structure as shown in Figure 5, where the molecules form a dimer pair which is arranged in a herring-bone manner, and short S...Se contacts of 3.66 and 3.68 Å are observed. The mobilities of the bottom-contact FETs of **16** and **17** are higher than those of **13** and **15**. Particularly, the mobilities at the substrate temperature of 25 °C are greatly increased by the introduction of the selenophene rings. The threshold voltages of the selenophene-containing compounds **16** and **17** are lower than those of **13** and **15** because of the higher electron affinity of the former. The mobilities were improved by increasing the substrate temperature, and the highest mobilities of **16** and **17** in the bottom-contact devices reached to 0.19 and 0.16 cm² V⁻¹ s⁻¹ at 100 °C, respectively.

4. Pyrazine-containing Compounds

Since pyrazine is a stronger electron acceptor than thiazole, compounds containing pyrazine units have been used as n-type semiconductors. Co-oligomers **18** and **19** with the pyrazine ring were easily prepared by the Stille coupling of 2-bromo-5-iodopyrazine with the corresponding stannyl reagents.¹⁵ They afforded n-type FETs, where the electron mobility was improved by replacing the thienyl unit with the thiazole one as shown in Table 3. This replacement also decreases the threshold voltage owing to the increase of electron affinity. Single-crystal structure analysis of **18** was carried out, which reveals the molecular structure with the N of the pyrazine and the S of thiophene in the same direction probably resulting from the electrostatic interaction. The crystal structure is a herringbone type which is different from the π -stacking structure of thiazolothiazole derivative **6**.

On the other hand, dicyanopyrazinopyridine **20** and its derivatives are strong electron acceptors.¹⁶ Various derivatives have been used as semiconductors for FETs. Although most of them showed n-type behavior, the electron mobilities were low (ca. 10⁻⁶ cm² V⁻¹ s⁻¹). This is probably due to the carrier trap by the cyano groups. Phenanthroline-fused pyrazine derivatives have high electron affinity stemming from the presence of four C=N double bonds. Such compounds were expected to show n-type semiconducting behavior without CN groups. In fact, terthiophene derivative **21** afforded an n-type FET. Interestingly, the quinquethiophene derivative **22** showed clear ambipolar FET characteristics, where both p- and n-type behaviors were observed.¹⁷ This is attributed to the increased HOMO level of **22**. Compound **22** has an absorption maximum at 727 nm resulting from the small HOMO–LUMO energy gap.

Tetrathiafulvalene (TTF) is a strong electron donor and its derivatives have been used as p-type semiconductors for OFETs. The HOMO levels of TTFs are very high, resulting in lability to oxygen. To decrease the HOMO levels, electron-accepting pyrazine rings were introduced. As a result, TTF derivative **23** containing fused-quinoxaline rings enhanced the air-stability.¹⁸ However, the compound still showed p-type behavior. In contrast, halogen-substituted derivatives **24** and **25** (Scheme 5) showed n-type behavior. Both of them showed a good electron mobility of 0.1 cm² V⁻¹ s⁻¹, and they became the first examples of n-type FETs based on TTF derivatives.¹⁹ The molecules are π -stacked to form columns as shown in Figure 6, which are dif-

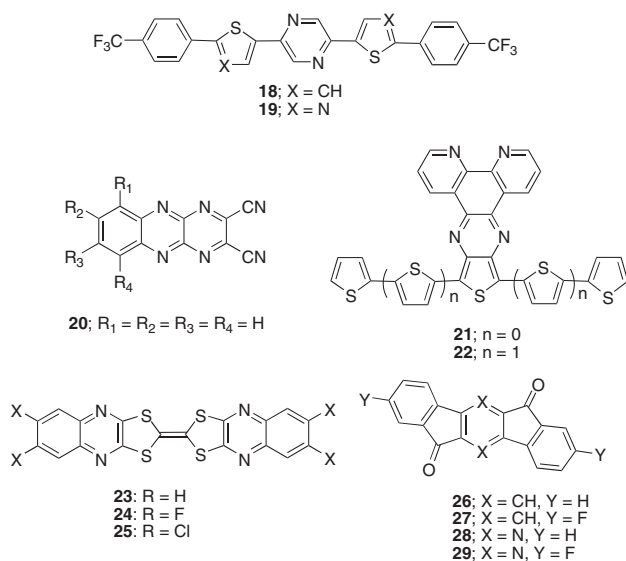
Figure 5. Crystal structure of **16**.**Table 3.** Reduction potentials and FET characteristics^a of pyrazine-containing compounds

Compound	E_{red} /V ^b	Device type	Mobility /cm ² V ⁻¹ s ⁻¹	Threshold /V
18	-1.86	bottom	8.3×10^{-4}	+105
19	-1.76	bottom	3.0×10^{-3}	+41
		top	0.04	+36
20	-0.03	bottom	3×10^{-6}	+4
21	-0.92	bottom	2×10^{-4}	+85
22	-0.83	bottom	(n) 6×10^{-5} (p) 1×10^{-5}	— ^c — ^c
23	< -1.9	top	(p) 0.20	-36
24	< -1.9	top	0.10	+49
25	< -1.9	top	0.11	+52
26	-1.19	top	not observed	
27	-1.02	bottom	0.17	+69
		top	6.6×10^{-2}	+75
28	-0.85	bottom	2.7×10^{-4}	+70
27	-0.75	bottom	1.1×10^{-2}	+27
		top	0.17	+17

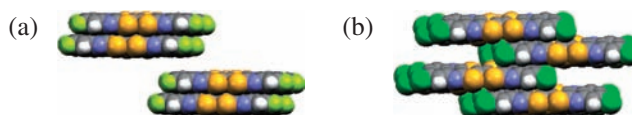
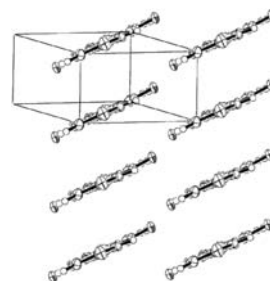
^aThe highest mobilities reported. ^bThe first reduction potentials, V vs. SCE. ^cNot reported.

ferent from a herringbone structure of a naphthalene-fused TTF.¹⁸ This can be attributed to the intermolecular charge-transfer interactions. The fluoro derivative **24** has an interaction between the electron-donating TTF unit and the electron-accepting quinoxaline part similarly to **23**, whereas in **24** the electron-withdrawing Cl atoms are sandwiched between the TTF units. The structure of **24** is a kind of 2-D column. In addition, both of them have short S...S contacts (3.56 and 3.60 Å) between the columns, forming a 2-D network. The effect of halogen substituents on the FET behavior was rationalized by the lower LUMO levels caused by the halogen atoms. This result confirms that the FET polarity can be determined by the frontier orbital energies of semiconductors and that end substituents can control the polarity.

Electron-accepting carbonyl compounds are candidates for n-type semiconductors as noted for anthraquinones **11** and **12**. Indenofluorenone derivatives **26** and **27** (Scheme 5) were expected to be semiconductors because of the planar rigid terphenylene structures, which are easily obtained from terephthalic acids. The pyrazine analogues **28** and **29** were synthesized from the corresponding indanone derivatives.²⁰ Single-crystal X-ray structure analyses of the fluoro derivatives **27** and **29** revealed



Scheme 5.

Figure 6. (a) Crystal structures of **24** and (b) **25**.Figure 7. Crystal structure of **27**.

the π -stacking columnar structures. The crystal structure of **27** is shown in Figure 7. The pyrazine derivatives have higher electron affinity than the corresponding benzene derivatives. The fluoro derivative **27** exhibited a high electron mobility of $0.17 \text{ cm}^2 \text{ V}^{-1} \text{ s}^{-1}$ in the bottom-contact FET although nonsubstituted **26** showed no FET characteristics. On the other hand, non-substituted pyrazine derivative **28** afforded an n-type FET and the FET of fluoro derivative **29** showed higher mobility. It should be noted here that the threshold voltage was much decreased by introduction of the pyrazine ring to **17** from 75 V in the top-contact devices. This can be attributed to smooth electron injection from the Au electrodes in **29** with higher electron affinity.

5. Summary

We have developed various n-type semiconductors composed of nitrogen-containing heterocycles. Introduction of the heterocyclic rings could control the LUMO levels and intermolecular interactions. Consequently, some of them afforded high electron mobilities, high on/off ratios, and low threshold voltages.

es. However, n-type FETs are generally unstable in air and the FET characteristics described here were measured under vacuum conditions. In addition, these devices were fabricated by vacuum evaporation of organic semiconductors since they have low solubility in solvents. To overcome those disadvantages, further studies are under way.

References

- 1 Y. Sun, Y. Liu, D. Zhu, *J. Mater. Chem.* **2005**, *15*, 53; A. R. Murphy, J. M. J. Fréchet, *Chem. Rev.* **2007**, *107*, 1066; J. E. Anthony, *Angew. Chem., Int. Ed.* **2008**, *47*, 452; S. Allard, M. Forster, B. Souharce, H. Thiem, U. Scherf, *Angew. Chem., Int. Ed.* **2008**, *47*, 4070.
- 2 H. Klauk, M. Halik, U. Zschieschang, F. Eder, G. Schmid, C. Dehm, *Appl. Phys. Lett.* **2003**, *82*, 4175; K. Takimiya, H. Ebata, K. Sakamoto, T. Izawa, T. Otsubo, Y. Kunugi, *J. Am. Chem. Soc.* **2006**, *128*, 12604; H. Ebata, T. Izawa, E. Miyazaki, K. Takimiya, M. Ikeda, H. Kuwabara, T. Yui, *J. Am. Chem. Soc.* **2007**, *129*, 15732; T. Yamamoto, K. Takimiya, *J. Am. Chem. Soc.* **2007**, *129*, 2224.
- 3 C. D. Dimitrakopoulos, P. R. L. Malenfant, *Adv. Mater.* **2002**, *14*, 99.
- 4 Z. Bao, A. J. Lovinger, J. Brown, *J. Am. Chem. Soc.* **1998**, *120*, 207; A. Facchetti, M. Mushrush, H. E. Katz, T. J. Marks, *Adv. Mater.* **2003**, *15*, 33; Y. Sakamoto, T. Suzuki, M. Kobayashi, Y. Gao, Y. Fukai, Y. Inoue, F. Sato, S. Tokito, *J. Am. Chem. Soc.* **2004**, *126*, 8138; M. L. Tang, A. D. Reichardt, P. Wei, Z. Bao, *J. Am. Chem. Soc.* **2009**, *131*, 5264.
- 5 S. Ando, J. Nishida, H. Tada, Y. Inoue, S. Tokito, Y. Yamashita, *J. Am. Chem. Soc.* **2005**, *127*, 5336.
- 6 S. Ando, R. Murakami, J. Nishida, H. Tada, Y. Inoue, S. Tokito, Y. Yamashita, *J. Am. Chem. Soc.* **2005**, *127*, 14996.
- 7 S. Ando, J. Nishida, Y. Inoue, S. Tokito, Y. Yamashita, *J. Mater. Chem.* **2004**, *14*, 1787.
- 8 D. Kumaki, S. Ando, S. Shimono, Y. Yamashita, T. Umeda, S. Tokito, *Appl. Phys. Lett.* **2007**, *90*, 053506.
- 9 M. Mamada, J. Nishida, D. Kumaki, S. Tokito, Y. Yamashita, *Chem. Mater.* **2007**, *19*, 5404.
- 10 M. Mamada, J. Nishida, S. Tokito, Y. Yamashita, *Chem. Lett.* **2008**, *37*, 766.
- 11 M. Mamada, J. Nishida, S. Tokito, Y. Yamashita, *Chem. Commun.* **2009**, 2177.
- 12 T. Kono, D. Kumaki, J. Nishida, T. Sakanoue, M. Kakita, H. Tada, S. Tokito, Y. Yamashita, *Chem. Mater.* **2007**, *19*, 1218.
- 13 M. Akhtaruzzaman, N. Kamata, J. Nishida, S. Ando, H. Tada, M. Tomura, Y. Yamashita, *Chem. Commun.* **2005**, 3183.
- 14 Y. Yamashita, S. Shimono, T. Kono, D. Kumaki, J. Nishida, S. Tokito, *Proc. SPIE* **2007**, 6658, 66580N-1.
- 15 T. Kojima, J. Nishida, S. Tokito, H. Tada, Y. Yamashita, *Chem. Commun.* **2007**, 1430.
- 16 J. Nishida, Naraso, S. Murai, E. Fujiwara, H. Tada, M. Tomura, Y. Yamashita, *Org. Lett.* **2004**, *6*, 2007.
- 17 J. Nishida, S. Murakami, H. Tada, Y. Yamashita, *Chem. Lett.* **2006**, *35*, 1236.
- 18 Naraso, J. Nishida, S. Ando, J. Yamaguchi, K. Itaka, H. Koinuma, H. Tada, S. Tokito, Y. Yamashita, *J. Am. Chem. Soc.* **2005**, *127*, 10142.
- 19 Naraso, J. Nishida, D. Kumaki, S. Tokito, Y. Yamashita, *J. Am. Chem. Soc.* **2006**, *128*, 9598.
- 20 T. Nakagawa, D. Kumaki, J. Nishida, S. Tokito, Y. Yamashita, *Chem. Mater.* **2008**, *20*, 2615.